Nanoscale Research Letters
a SpringerOpen Journal

NANO EXPRESS   **Open Access**

Near-infrared emitting $CdTe_{0.5}Se_{0.5}/Cd_{0.5}Zn_{0.5}S$ quantum dots: synthesis and bright luminescence

Ping Yang[1,2], Shiquan Wang[1] and Norio Murase[1*]

Abstract

We present how $CdTe_{0.5}Se_{0.5}$ cores can be coated with $Cd_{0.5}Zn_{0.5}S$ shells at relatively low temperature (around 200°C) via facile synthesis using organic ammine ligands. The cores were firstly fabricated via a less toxic procedure using CdO, trioctylphosphine (TOP), Se, Te, and trioctylamine. The cores with small sizes (3.2-3.5 nm) revealed green and yellow photoluminescence (PL) and spherical morphologies. Hydrophobic core/shell $CdTe_{0.5}Se_{0.5}/Cd_{0.5}Zn_{0.5}S$ quantum dots (QDs) with tunable PL between green and near-infrared (a maximum PL peak wavelength of 735 nm) were then created through a facile shell coating procedure using trioctylphosphine selenium with cadmium and zinc acetate. The QDs exhibited high PL efficiencies up to 50% because of the formation of a protective $Cd_{0.5}Zn_{0.5}S$ shell on the $CdTe_{0.5}Se_{0.5}$ core, even though the PL efficiency of the cores is low (≤1%). Namely, the slow growth process of the shell plays an important role for getting high PL efficiencies. The properties of the QDs are largely determined by the properties of $CdTe_{0.5}Se_{0.5}$ cores and shells preparation conditions such as reaction temperature and time. The core/shell QDs exhibited a small size diameter. For example, the average diameter of the QDs with a PL peak wavelength of 735 nm is 6.1 nm. Small size and tunable bright PL makes the QDs utilizable as bioprobes because the size of QD-based bioprobes is considered as the major limitation for their broad applications in biological imaging.

Keywords: Quantum dots, Semiconductor, Photoluminescence, Near-infrared, Core/shell

Background

Semiconductor quantum dots (QDs) have attracted considerable interest in the past decade because of their excellent properties such as narrow, symmetric, and tunable emission spectra, broad absorption spectra, superior photostability, high photoluminescence (PL) efficiency, and the capacity of simultaneous excitation of multiple fluorescence colors compared with the organic dyes and fluorescent proteins [1-4]. Moreover, the near-infrared (NIR) spectral range presents many advantages for *in vivo* fluorescence imaging. The absorption of photons by biological tissues is much reduced in this spectral window compared with the visible range. There are many more alternatives in QDs with NIR emission for *in vivo* imaging than organic dyes [5]. For example, the QDs with a PL of 700-nm region minimize the problems of indigenous fluorescence of tissues and meet the requirements of *in vivo* biological imaging applications. Therefore, the synthesis of NIR-emitting QDs (700–900 nm) has received much attention recently. In addition, the QDs have advantages compared with metallic nanoparticles for nanoprobes because of their broad absorption band and tunable and bright PL [6].

CdSe is still one of the most popular QDs created by various chemical strategies. However, CdSe (E_g = 1.76 eV, a_B = 9.6 nm) QDs can be tuned through quantum confinement to emit visible fluorescent spectrum only reaching typically 650–700 nm. Furthermore, it is difficult to grow CdSe-based QDs with NIR emission because of their growth kinetics. In addition, the size of CdSe with a longer PL peak wavelength becomes too large for bioprobers. Compared with CdSe, the band gap of bulk CdTe is narrow (1.56 eV, corresponding to approximately 795 nm wavelength). The PL peak wavelength of CdTe QDs with a diameter of 7 nm can reach approximately 720 nm. However, CdTe and CdTe/CdSe QDs prepared by an organic synthesis are normally unstable, which results in low PL efficiency and fast

* Correspondence: n-murase@aist.go.jp
[1]Health Research Institute, National Institute of Advanced Industrial Science & Technology (AIST), Hayashi-cho, Takamatsu-city, Kagawa 761-0395, Japan
Full list of author information is available at the end of the article

Springer

photobleaching. Therefore, composited CdTe and CdSe QDs or CdTe-based QDs with protective inorganic shells are expected. Especially, these QDs with NIR emission and small size are necessary. However, there have been few reports of a higher band gap shell growth around CdTe or CdTeSe QDs. Rogach and co-workers described the aqueous synthesis of 8–10 nm CdTe-based QDs emitting at approximately 800 nm [7].

For a purpose of getting a highly stable fabricating CdTeSe-composited cores with a higher band gap shell is still a challenge. Nanoalloying of two semiconductors shows properties distinct not only from the properties of their bulk counterparts (such as $CdTe_{0.5}Se_{0.5}$), but also from those of their parent semiconductors (such as CdTe or CdSe). Engineering the band gap energy of QDs has resulted in the development of core/shell QDs with novel exciting properties and applications. Recently, Jiang et al. reported that they were able to deposit only a very thin CdS shell (approximately one monolayer) on the surface of a CdTeSe core [8]. However, the band gap of CdS is not large enough to provide the potential barrier necessary to block both electrons and holes inside CdTeSe cores. A ZnS shell has a crucial role in the improvement of PL properties of QDs. This increases the chemical stability and photostability of the QDs because ZnS is a chemically stable with wide band gap (3.8 eV for the bulk material) semiconductor material. However, the large mismatch between CdTeSe and ZnS lattice parameters enables the strain at the interface between the core and the shell. Therefore, a $Cd_xZn_{1-x}S$ composite shell can also improve the stability and PL properties of the QDs. Very recently, we fabricated CdSe cores coated with $Cd_xZn_{1-x}S$ composite shells [9]. These core/shell QDs reveal broadly tunable PL spectra (PL peak wavelength up to 650 nm), narrow size distribution, high PL efficiency (up to 60%, in the case of CdSe cores with a PL efficiency of 1%), and a high stability (keeping their initial PL efficiency in a toluene solution for 1 year).

To reduce the lattice parameter mismatch and improve the properties of core/shell QDs, an interlayer is inserted, such as CdS and ZnSe between the CdSe core and ZnS shell. A $Cd_xZn_{1-x}S$ composite shell has led to the formation of CdS interlayer due to the growth kinetics of CdS and ZnS. Thus, CdTeSe cores would strongly benefit from $Cd_xZn_{1-x}S$ composite shells for getting a longer PL peak wavelength, as well as high stability and PL efficiency. However, very little reports focused on the NIR emission of composite cores coated with a higher band gap composited shell. Recently, Pons et al. reported that near-infrared-emitting CdTeSe/CdZnS core/shell QDs prepared using cadmium oxide (CdO), zinc oxide (ZnO), tetradecylphosphonic acid (TDPA), cadmium oleate ($Cd(OA)_2$), and zinc oleate ($Zn(OA)_2$) as precursors

revealed a high stability [10]. Because of decreased lattice mismatch between the core and the shell, the interface strain decreases dramatically during the shell growth, indicating that the spatial distribution of defects in core/shell QDs can be controlled by the shell growth. A better understanding of the shell effect on optical properties of QDs is important for optimizing the synthesis. Because Cd-based QD is undesirable for biological imaging due to toxicity, a CdZnS shell with a ZnS-rich layer coated on the surface of CdSe is used to decrease the release of Cd ions in this paper. We further have a technique of glass coating on the surface of the QDs as well for the purpose of drastically reducing the amount of Cd released from the QDs as demonstrated in the previous publications [11,12].

For the preparation of QDs by classical colloidal chemistry, organometallic and/or metal organic compounds under anaerobic conditions have been employed. For example, CdSe QDs were prepared by reacting dimethylcadmium ($CdMe_2$) with trioctylphosphine selenium (TOP)Se in TOP/trioctylphosphine oxide or TOPO at high temperature [13]. Therefore, a novel and facile synthesizing strategy, which uses a faster reaction process and less toxic chemicals, is highly desirable. To address a novel method for fabricating QDs with NIR PL, more efforts to other potential preparation methods of QDs have been taken in our group. In this paper, $CdTe_{0.5}Se_{0.5}/Cd_{0.5}Zn_{0.5}S$ core/shell QDs were fabricated using less toxic chemicals and a facile synthesis. These core/shell QDs revealed tunable PL peak wavelength from the initial value of $CdTe_{0.5}Se_{0.5}$ cores to 735 nm with much improved PL efficiency above 50%. A detailed consideration allows us to grow multilayer $Cd_{0.5}Zn_{0.5}S$ shell around $CdTe_{0.5}Se_{0.5}$ QDs using air stable zinc and cadmium acetate precursors at relatively low temperature (approximately 200°C). The resulting core/shell QDs exhibit improved stability and PL efficiency compared with $CdTe/Cd_{0.5}Zn_{0.5}S$ QDs.

Methods
Chemicals
All chemicals were of analytical grade or of the highest purity available and used directly without any further purification. Cadmium oxide (CdO, 99.99%), cadmium acetate dihydrate ($Cd(Ac)_2 2H_2O$, 98%), zinc acetate ($Zn(Ac)_2$, 99.99%), selenium (Se, 99.5%), sulfur (S, 99.98%, powder), tellurium (Te, 99.99%), octadecylphosphonic acid (ODPA, 97%), trioctylamine (TOA, 98%), octadecene (ODE, technical grade of 90%, ODE), TOP (97%), hexadecylamine (HDA), and TOA were supplied by Sigma Aldrich (St. Louis, MO, USA). The pure water was obtained from a Milli-Q synthesis system (resistivity of 18.2 MΩ·cm) (EMD Millipore Corporation, Billerica, MA, USA).

Preparation of CdTe$_{0.5}$Se$_{0.5}$, CdSe, and CdTe cores

All preparations were carried out under N$_2$ atmosphere. A typical CdTe$_{0.5}$Se$_{0.5}$ core synthesis is composed of one-step growth as described hereafter. A 0.54 mmol of CdO and 180 mg of ODPA were mixed with 7 mL of TOA in a three-neck round-bottom flask under N$_2$ flow, and stirred at 140°C for 1 h to remove adsorbed H$_2$O. Then the mixture was kept at 280°C until the CdO completely dissolved. A 0.5 mmol of Se powder and Te powder were completely dissolved in 1 mL of TOP with stirring. The TOPSe with TOPTe solution was then swiftly injected into the cadmium precursor solution with stirring, and kept at 280°C for 2 min, followed by cooling down to room temperature. A 10 mL of hexane and 50 mL of ethanol were added to precipitate as-prepared samples. The resulting sample was then washed with copious ethanol, re-dispersed in 20 mL of toluene, and centrifuged at 12,000 rpm for 5 min to remove the sludge. Next the cores were precipitated with ethanol and re-dispersed in 10 mL of toluene for subsequent shell coating. To prepare CdTe$_{0.5}$Se$_{0.5}$ cores with various sizes, the reaction time and temperature as well as the injection speed of TOPSe and TOPTe were adjusted. The preparation conditions and properties of CdTe$_{0.5}$Se$_{0.5}$ cores and CdTe$_{0.5}$Se$_{0.5}$/Cd$_{0.5}$Zn$_{0.5}$S core/shell QDs are summarized in Table 1.

Alternatively, CdSe cores were fabricated by injecting 1 mL of TOPSe with 1 mmol Se in the precursor of Cd within 30 s under N$_2$ flow. After further reaction for 2 min, the resulting sample was separated by using a similar procedure with that of CdTe$_{0.5}$Se$_{0.5}$ cores. CdTe cores were synthesized by addition of 1 mL of TOPTe with 1 mmol Te within 30 s under N$_2$ flow. The CdTe cores were precipitated twice in ethanol and resuspended in 10 mL of toluene.

Preparation of CdTe$_{0.5}$Se$_{0.5}$ and CdTe cores coated with Cd$_{0.5}$Zn$_{0.5}$S shell

The preparation of Cd$_{0.5}$Zn$_{0.5}$S shell was carried out by directly reacting cadmium and zinc acetate with TOPS. In a typical synthesis, 14 mg of Cd(Ac)$_2$2H$_2$O, 10 mg of Zn(Ac)$_2$, 0.5 g of HDA, and 5 mL of ODE were mixed in a three-neck round-bottom flask under N$_2$ flow and stirred at 200°C until the Cd and Zn salts were completely dissolved. A 6 mg of S powder was dissolved in 0.5 mL of TOP. The toluene solution of CdTe$_{0.5}$Se$_{0.5}$ or CdTe cores (3 mL) was injected with vigorous stirring followed by the injection of the TOPS solution. The mixture was kept at 200°C with stirring for several to several 10 min, followed by cooling down to room temperature. The products were precipitated, washed twice with ethanol, and re-dispersed in 10 mL of toluene. To investigate the effect of preparation conditions on properties, reaction time and temperature were adjusted.

Apparatus

The transmission electron microscopy (TEM) observations of samples were performed mainly using a Hitachi EF-1000 electron microscope (Hitachi Ltd., Tokyo, Japan). The absorption and PL spectra were recorded using conventional spectrometers (Hitachi U-4000 and F-4500, respectively). Both excitation and emission slits are 5 nm for the measurement of PL spectra. The PL efficiencies of samples in solution were estimated using a method previously reported [14]. Briefly, the PL and absorption spectra of a standard quinine solution (quinine in 0.1 N H$_2$SO$_4$ solution; PL efficiency η_0 of 55%) were measured in a 1-cm quartz cell as a function of the concentration.

Results and discussion

Alloyed semiconductor QDs can be classified as having whether (1) a uniform internal structure (i.e., homogeneous) or (2) a gradient internal structure, where the alloy composition varies in different parts of the QD [15,16]. The structure of these QDs differs from that of core/shell QDs, where a thin layer of a wider band gap semiconductor is grown on the surface of a core semiconductor. The properties of alloyed QDs are characterized by Végard's law which states that while lattice constant changes linearly with composition, other physical properties such as band gap often vary nonlinearly. In the case of QDs of any composition, quantum confinement also dictates size dependence [17] as shown in this equation:

$$E_g(d) = E_g(\infty) + \frac{a}{d} + \frac{c}{d^2},$$

where d is the QD diameter and a and c are empirical fit parameters. Since the PL properties of QDs depended

Table 1 Preparation conditions and properties of CdTe$_{0.5}$Se$_{0.5}$ cores and CdTe$_{0.5}$Se$_{0.5}$/Cd$_{0.5}$Zn$_{0.5}$S core/shell QDs

Sample	Reaction time (min)	Reaction temperature (°C)	Composition	PL peak wavelength (nm)	PL efficiency (%)	FWHM (nm)
1	2.5	280	CdTe$_{0.5}$Se$_{0.5}$	573.4	0.9	23.6
2[a]	6	220	CdTe$_{0.5}$Se$_{0.5}$/Cd$_{0.5}$Zn$_{0.5}$S	700.4	48.3	65.2
3	2.5	280	CdTe$_{0.5}$Se$_{0.5}$	576.4	1.1	38.4
4[a]	11	200	CdTe$_{0.5}$Se$_{0.5}$/Cd$_{0.5}$Zn$_{0.5}$S	656.2	52.2	64.4

[a]These samples were prepared by using samples 1 and 3, respectively.

strongly on their band gap and size, the alloyed $CdTe_{0.5}Se_{0.5}$ QDs revealed different PL properties compared with CdTe and CdSe QDs.

The quantum confinement of QDs with any composition dictates size dependence. Similar to bulk $CdTe_xSe_{1-x}$ alloy, a very slight nonlinear relationship between the band gap energy and the composition, known as 'optical bowing', was also observed for the QDs. For example, Han's group reported similar observations for homogeneous $Zn_xCd_{1-x}S$ QDs. To investigate the effect of composition on PL properties, we prepared three kinds of QDs including $CdTe_{0.5}Se_{0.5}$, CdTe, and CdSe by using the same preparation procedure as indicated in 'Methods' section. Table 2 summarizes the property comparison of CdTe, CdSe, and $CdTe_{0.5}Se_{0.5}$ QDs. $CdTe_{0.5}Se_{0.5}$ QDs revealed a longer PL peak wavelength and smaller size than those of CdSe QDs. Compared with CdTe QDs, alloyed $CdTe_{0.5}Se_{0.5}$ QDs can provide better stability because of Se. In our experiment the PL of as-prepared CdTe QDs was quenched after 2 days. In contrast, both of CdSe and $CdTe_{0.5}Se_{0.5}$ QDs kept their initial PL efficiency after 1 month.

The size of QDs depended strongly on preparation conditions. To create $CdTe_{0.5}Se_{0.5}$ cores with various sizes, reaction time and the injection speed of TOPSe and TOPTe were adjusted. The PL spectra of $CdTe_{0.5}Se_{0.5}$ cores red-shifted with time under a low injection speed. This is ascribed to the reaction time and concentration dependence of precursor for the nucleation and growth of the cores. As summarized in Tables 1, 3, and 4, the PL peak wavelength of the cores was 573 to 592 nm.

Because CdSe/CdS QDs have less lattice mismatch (approximately 3.9%) than that of CdSe/ZnS QDs (approximately 12%) [18,19], an alloy $Cd_xZn_{1-x}S$ shell can provide better stability by decreasing interfacial strain between cores and shells. Quyang et al. reported that gradiently alloyed $Zn_xCd_{1-x}S$ QDs having a Cd-rich core and Zn-rich shell could be synthesized via a noninjection one-pot approach [20]. In our experiments $CdTe_{0.5}Se_{0.5}$ cores were coated with $Cd_{0.5}Zn_{0.5}S$ composite shell by an organic one-step synthesis. The shell layers of CdS and ZnS might not be clearly separated, and it is also possible that the shell layer is a gradient alloy structure of CdS and ZnS. This is ascribed to the growth kinetic

Table 2 Property comparison of CdTe, CdSe, and $CdTe_{0.5}Se_{0.5}$ QDs

Composition	PL peak wavelength (nm)	Diameter (nm)
CdTe	550	2.8
CdSe	544	4.0
$CdTe_{0.5}Se_{0.5}$	570	3.2

Table 3 Preparation condition and properties of $CdTe_{0.5}Se_{0.5}/Cd_{0.5}Zn_{0.5}S$ QDs

Sample	Reaction time(min)	PL peak	PL efficiency	FWHM (nm)
5[a]	N/A	588.2	0.9	21.4
5-1	1	589.4	36.2	44.2
5-2	2	603.4	44.2	56.4
5-3	3	611.0	46.2	62.2
5-4	5	614.4	48.9	67.4
5-5	7	621.6	52.5	67.4
5-6	10	630.4	51.6	67.6
5-7	15	643.8	43.0	71.6
5-8	20	663.4	44.4	77.0
5-9	35	683	38.9	86.0

[a]The core/shell QDs were prepared by using sample 5. The properties of $CdTe_{0.5}Se_{0.5}$ cores are listed for comparison.
N/A not available.

of CdS and ZnS. The gradient structure would be beneficial to improve stability by reducing lattice mismatch between CdSe and ZnS layers.

According to our previous experimental results, an optimal molar ratio of Cd/Zn of 1/1 was used for $CdTe_{0.5}Se_{0.5}$ cores coated with $Cd_{0.5}Zn_{0.5}S$ shell for getting high PL efficiencies. To investigate the effect of temperature on the formation of $Cd_{0.5}Zn_{0.5}S$ shell on $CdTe_{0.5}Se_{0.5}$ cores, reaction temperature was adjusted from 180°C to 280°C. An optimal temperature range was found to be around 190°C to 220°C. In the case of a high temperature (more than 260°C), the reaction solution became black quickly when TOPS was injected. This is ascribed to the PL quenching of QDs because the high temperature led to large amount defects generated

Table 4 Preparation condition and properties of $CdTe_{0.5}Se_{0.5}/Cd_{0.5}Zn_{0.5}S$ QDs

Sample	Reaction time(min)	PL peak	PL efficiency	FWHM (nm)
6[a]	N/A	592.4	1.0	39.4
6-1	3	611.2	7.7	47.6
6-2	6	639.6	19.9	55.4
6-3	9	653.6	21.9	55.4
6-4	12	664.4	26.9	57.8
6-5	15	674.4	15.0	62.8
6-6	18	682.8	19.7	67.4
6-7	21	692.2	28.5	73.0
6-8	25	702.6	48.9	80.4
6-9	30	716.6	45.85	92.0
6-10	35	735.2	40.54	94.2

[a]The core/shell QDs were prepared by using sample 6. The properties of $CdTe_{0.5}Se_{0.5}$ cores are listed for comparison.
N/A not available.

during preparation. Table 1 summarizes the preparation conditions and properties of $CdTe_{0.5}Se_{0.5}$ cores and $CdTe_{0.5}Se_{0.5}/Cd_{0.5}Zn_{0.5}S$ QDs.

Figure 1 shows the TEM images of $CdTe_{0.5}Se_{0.5}$ cores and $CdTe_{0.5}Se_{0.5}/Cd_{0.5}Zn_{0.5}S$ core/shell QDs shown in Table 1: (a) sample 1 ($CdTe_{0.5}Se_{0.5}$ cores), (b) sample 2 ($CdTe_{0.5}Se_{0.5}/Cd_{0.5}Zn_{0.5}S$) prepared by sample 1, (c) sample 3 ($CdTe_{0.5}Se_{0.5}$), and (d) sample 4 ($CdTe_{0.5}Se_{0.5}/Cd_{0.5}Zn_{0.5}S$) prepared by sample 3. Samples 2 and 4 were prepared at 220°C and 200°C, respectively. $CdTe_{0.5}Se_{0.5}$ cores revealed a spherical morphology (samples 1 and 3). In contrast, the core/shell QDs (samples 2 and 4) exhibited a tetrahedron-like morphology. This is ascribed to the CdS interlayer anisotropic deposition on $CdTe_{0.5}Se_{0.5}$ cores. For comparison, we fabricated $CdTe_{0.5}Se_{0.5}/ZnS$ QDs using a similar preparation procedure. The result indicates that $CdTe_{0.5}Se_{0.5}$ coated with a ZnS shell revealed a spherical morphology. This indicates the anisotropic deposition of CdS on the core occurs.

Figure 2 shows the absorption and PL spectra of $CdTe_{0.5}Se_{0.5}$ cores and core/shell $CdTe_{0.5}Se_{0.5}/Cd_{0.5}Zn_{0.5}S$ QDs shown in Table 1: (a) sample 1 ($CdTe_{0.5}Se_{0.5}$ cores), (b) sample 2 ($CdTe_{0.5}Se_{0.5}/Cd_{0.5}Zn_{0.5}S$ core/shell QDs), (c) sample 3 ($CdTe_{0.5}Se_{0.5}/Cd_{0.5}Zn_{0.5}S$ core/shell QDs), and (d) sample 4 ($CdTe_{0.5}Se_{0.5}/Cd_{0.5}Zn_{0.5}S$ core/shell QDs). A significant red shift was observed in both the absorption and PL spectra of the core/shell QDs in contrast to those of $CdTe_{0.5}Se_{0.5}$ cores. This is ascribed to the formation

Figure 1 TEM images of $CdTe_{0.5}Se_{0.5}$ cores and $CdTe_{0.5}Se_{0.5}/Cd_{0.5}Zn_{0.5}S$ core/shell QDs shown in Table 2. (a) Sample 1 ($CdTe_{0.5}Se_{0.5}$ cores), (**b**) sample 2 ($CdTe_{0.5}Se_{0.5}/Cd_{0.5}Zn_{0.5}S$) prepared by sample 1, (**c**) sample 3 ($CdTe_{0.5}Se_{0.5}$), and (**d**) sample 4 ($CdTe_{0.5}Se_{0.5}/Cd_{0.5}Zn_{0.5}S$) prepared by sample 3.

of a $CdTe_{0.5}Se_{0.5}/Cd_{0.5}Zn_{0.5}S$ core/shell structure. Being coated with a $Cd_{0.5}Zn_{0.5}S$ shell, the PL efficiency was drastically increased as shown in Table 1. However, the full width at half maximum (FWHM) of PL spectra was increased. This is because of the size distribution which became broad after coating with the shell.

For traditional QD synthesis by organic amine as a capping agent, researchers normally selected metal oleate and stearate as precursors. The combination of precursor and ligand is important for the non-coordinating solvent system. Metal stearate is a relatively stable precursor that could be coheated with a higher ratio of alkylamines such as 1-octadecylamine and HDA at high temperature (280°C-320°C) [20]. In contrast nucleation and growth in a metal oleate and HDA reaction system are executed at a moderate reaction temperature (265°C-285°C). In the present experiments, $CdTe_{0.5}Se_{0.5}$ cores were coated with $Cd_{0.5}Zn_{0.5}S$ shells using cadmium and zinc acetate as precursors to react with TOPS in ODE with HDA. The reaction temperature can be further lowered because of salt acetate with a short carbon chain. In addition the preparation of the core/shell QDs has to be carried out quickly to prevent the decomposition of salt acetate. Namely, cadmium and zinc acetate can be decomposed into CdO and ZnO if the solution was kept at a high temperature (more than 240°C) for a long time (more than 20 min). In contrast the reaction for the formation of QDs can be easily controlled at low temperature (less than 210°C). Because of a slow growth procedure, the core/shell QDs revealed a high PL efficiency as shown in Table 1.

To clarify the effect of reaction time on PL properties of $CdTe_{0.5}Se_{0.5}/Cd_{0.5}Zn_{0.5}S$ core/shell QDs, Table 3 summarizes the preparation condition and properties of $CdTe_{0.5}Se_{0.5}/Cd_{0.5}Zn_{0.5}S$ QDs prepared by sample 5 ($CdTe_{0.5}Se_{0.5}$ cores). The PL properties of sample 5 are listed for comparison. Figure 3 shows the PL peak wavelength and efficiency of $CdTe_{0.5}Se_{0.5}/Cd_{0.5}Zn_{0.5}S$ core/shell QDs (samples 5–1 to 5–9 shown in Table 3) versus reaction time. A gradual red shift of PL spectra was observed with time. This is ascribed to the thickness increase of the $Cd_{0.5}Zn_{0.5}S$ shell with prolonged reaction time. The FWHM of PL spectra was increased after coating with a $Cd_{0.5}Zn_{0.5}S$ shell. The formation of a $Cd_{0.5}Zn_{0.5}S$ shell around $CdTe_{0.5}Se_{0.5}$ cores resulted in a drastic improvement of PL efficiency (up to 52.5 % when the reflux time is 7 min). The PL efficiency of the core/shell QDs was decreased with further increasing the reflux time. This is ascribed to the lattice mismatch generated by increasing shell thickness.

The PL efficiency of QDs is significantly influenced by the QDs' surface state, such as the stoichiometric ratio of anion and cation, the nature and coverage ratio of the capping agent, and the polarity of the dispersing solvent

Figure 2 Absorption and PL spectra of CdTe$_{0.5}$Se$_{0.5}$ cores and CdTe$_{0.5}$Se$_{0.5}$/Cd$_{0.5}$Zn$_{0.5}$S core/shell QDs shown in Table 2. (**a**) Sample 1 (CdTe$_{0.5}$Se$_{0.5}$ cores), (**b**) sample 2 (CdTe$_{0.5}$Se$_{0.5}$/Cd$_{0.5}$Zn$_{0.5}$S Core/shell QDs), (**c**) sample 3 (CdTe$_{0.5}$Se$_{0.5}$/Cd$_{0.5}$Zn$_{0.5}$S core/shell QDs), and (**d**) sample 4 (CdTe$_{0.5}$Se$_{0.5}$/Cd$_{0.5}$Zn$_{0.5}$S Core/shell QDs). Samples 2 and 4 were prepared by using samples 1 and 3, respectively.
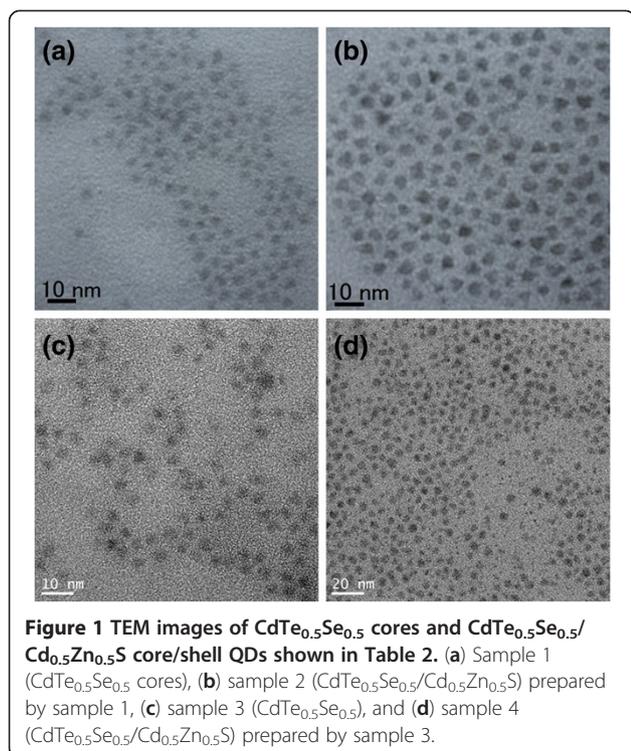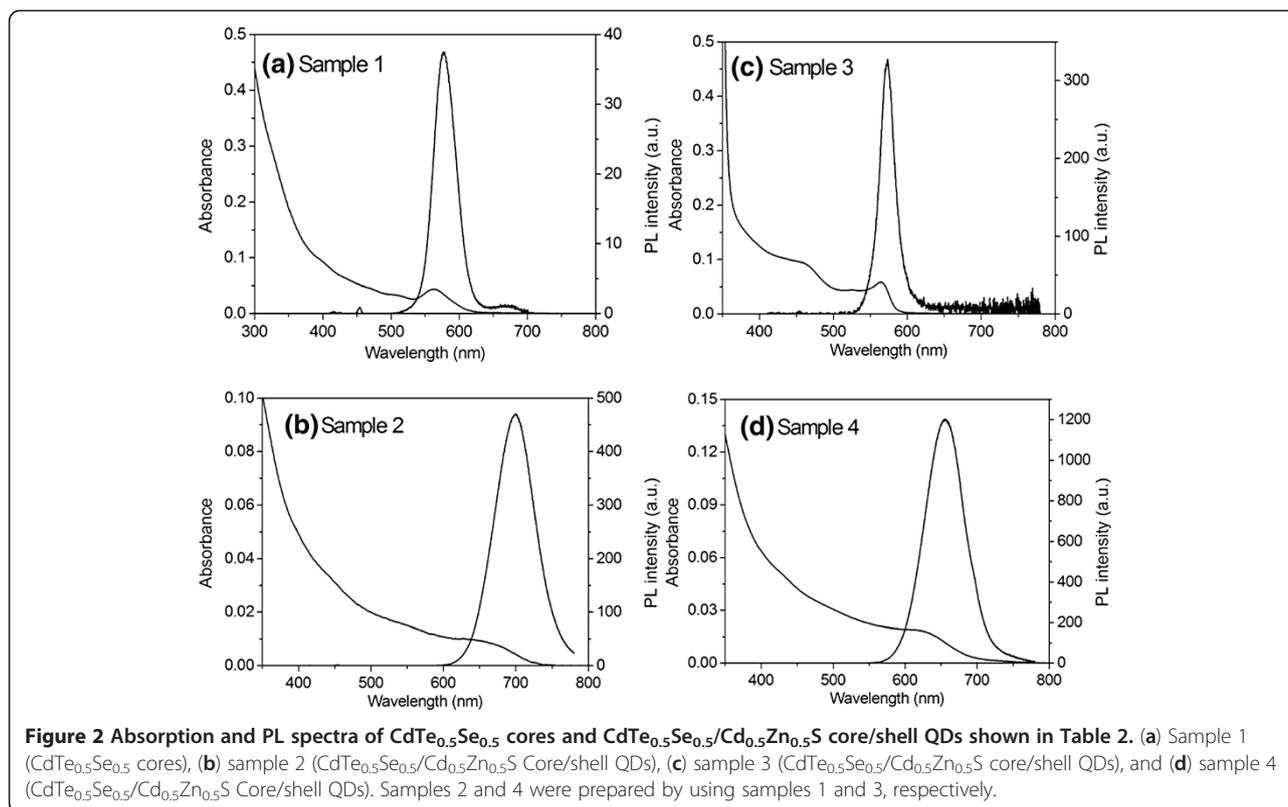
[21]. In order to stabilize and maximize PL, a semiconductor shell with higher band gap not only passivates the surface bonds but also varies the semiconductor potential energy well, concentrating the charge carriers in a core away from the surface [22,23]. Thereby, surface defect states and trap sites will have a diminished impact on the PL efficiency, and fewer environmental factors will influence the emission intensity. At the beginning of

Figure 3 PL peak wavelength and efficiency of CdTe$_{0.5}$Se$_{0.5}$/Cd$_{0.5}$Zn$_{0.5}$S core/shell QDs (Samples 5–1 to 5–9 shown in Table 3) versus reaction time. The core/shell QDs were prepared by sample 5. Star in the figure shows efficiency, while white square shows PL peak wavelength.

a shell coating, the passivation of a surface led a quick increase of PL efficiency. When the shell grew to a desired thickness, the corresponding PL efficiency of the resulting core/shell QDs approached the maximum value.

To confirm the increase of shell thickness with time, Figure 4 shows the TEM images of CdTe$_{0.5}$Se$_{0.5}$ cores and CdTe$_{0.5}$Se$_{0.5}$/Cd$_{0.5}$Zn$_{0.5}$S core/shell QDs shown in Table 3: (a) sample 5 (CdTe$_{0.5}$Se$_{0.5}$), (b) sample 5–4 (CdTe$_{0.5}$Se$_{0.5}$/Cd$_{0.5}$Zn$_{0.5}$S), (c) sample 5–8 (CdTe$_{0.5}$Se$_{0.5}$/ Cd$_{0.5}$Zn$_{0.5}$S), and (d) sample 5–9 (CdTe$_{0.5}$Se$_{0.5}$/ Cd$_{0.5}$Zn$_{0.5}$S). The average diameter of samples 5, 5–4, 5–8, and 5–9 is 3.3, 3.6, 4.7, and 5.3 nm, respectively. The shell thickness of 1 nm resulted in a large red shift of 75.2 nm of the PL spectrum. This is significantly different from that of a CdSe core coated with a Cd$_{0.5}$Zn$_{0.5}$S shell [6]. This is ascribed to the effect of band gap of core and shell on PL properties.

Because the size of CdTe$_{0.5}$Se$_{0.5}$ cores plays an important role for the PL properties of CdTe$_{0.5}$Se$_{0.5}$/Cd$_{0.5}$Zn$_{0.5}$S core/shell QDs, we fabricated the core/shell QDs using a large core. Table 4 summarizes the preparation condition and properties of CdTe$_{0.5}$Se$_{0.5}$/Cd$_{0.5}$Zn$_{0.5}$S QDs by a large CdTe$_{0.5}$Se$_{0.5}$ core (sample 6). The PL properties of sample 6 are listed for comparison. Figure 5 shows the PL peak wavelength and efficiency of CdTe$_{0.5}$Se$_{0.5}$/ Cd$_{0.5}$Zn$_{0.5}$S core/shell QDs (samples shown in Table 4) versus reaction time. A gradual red shift of PL spectra was observed with time. The FWHM of PL spectra was

Figure 4 TEM images of CdTe$_{0.5}$Se$_{0.5}$ cores and CdTe$_{0.5}$Se$_{0.5}$/ Cd$_{0.5}$Zn$_{0.5}$S core/shell QDs shown in Table 3. (**a**) Sample 5 (CdTe$_{0.5}$Se$_{0.5}$), (**b**) samples 5–4 (CdTe$_{0.5}$Se$_{0.5}$/Cd$_{0.5}$Zn$_{0.5}$S), (**c**) sample 5–8 (CdTe$_{0.5}$Se$_{0.5}$/Cd$_{0.5}$Zn$_{0.5}$S), and (**d**) sample 5–9 (CdTe$_{0.5}$Se$_{0.5}$/ Cd$_{0.5}$Zn$_{0.5}$S). Samples 5–4, 5–8, and 5–9 were prepared by using sample 5.
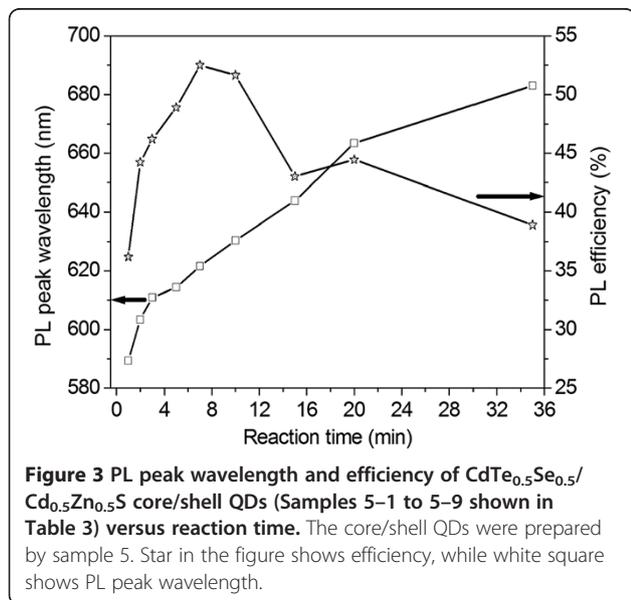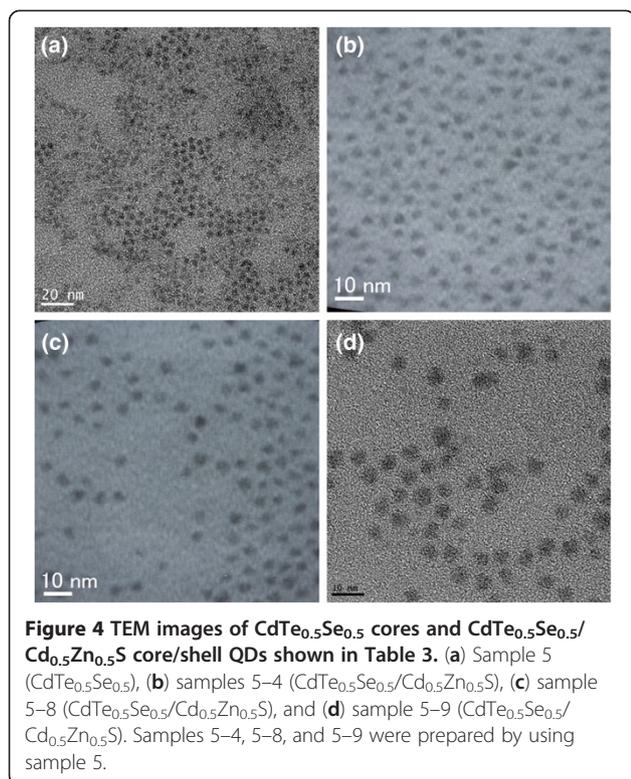
increased after coating with a Cd$_{0.5}$Zn$_{0.5}$S shell. Compared with samples 5–9 shown in Table 3, samples 6–10 revealed a longer PL peak wavelength (735 nm) even though they were prepared using the same reflux time (35 min). This is ascribed to the increase in the core size. Because samples 6–10 exhibited a PL efficiency of 40%, the large CdTe$_{0.5}$Se$_{0.5}$ core can be a good candidate for the preparation of QDs with NIR and mid-infrared

Figure 5 PL peak wavelength and efficiency of CdTe$_{0.5}$Se$_{0.5}$/ Cd$_{0.5}$Zn$_{0.5}$S core/shell QDs (Samples 6–1 to 6–10 shown in Table 4) versus reaction time. The core/shell QDs were prepared by using sample 6. White square in the figure shows the PL peak wavelength, while black circle shows PL efficiency.
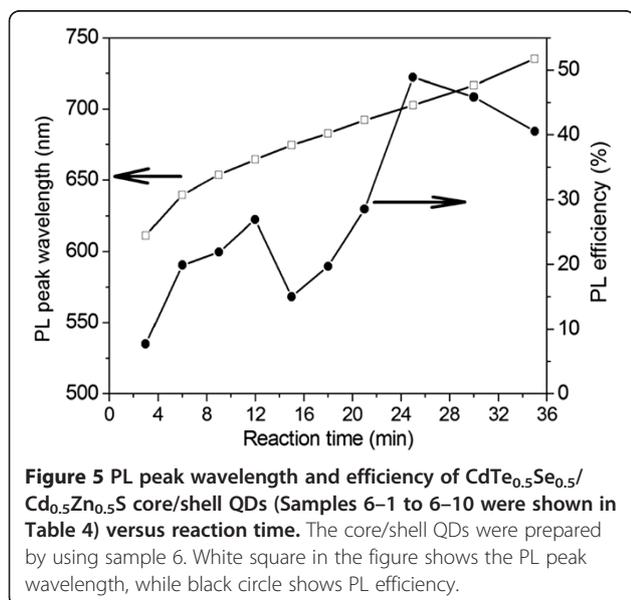
emission. Figure 6 shows the TEM images of CdTe$_{0.5}$Se$_{0.5}$/Cd$_{0.5}$Zn$_{0.5}$S core/shell QDs shown in Table 4: (a) sample 6–5 and (b) sample 6–9. Sample 6–5 revealed a much narrow size distribution than that of sample 6–9. Because a longer reflux time (sample 6–9) resulted in a broad size distribution as shown in Figure 6b, the FWHM of PL spectrum of sample 6–9 became large compared with that of sample 6–5 as shown in Table 4.

Generally, CdTe QDs show poor photostability because of the easy oxidation of tellurium as we have mentioned before. The stability was increased by being coated with a Zn$_{0.5}$Cd$_{0.5}$S shell. Especially in the case of CdTe$_{0.5}$Se$_{0.5}$ cores coated with a Cd$_{0.5}$Zn$_{0.5}$S shell, the core/shell QDs with a QD concentration of 100 nM in a toluene solution retained their initial PL efficiency for 1 month.

Conclusions

A successful approach for preparing highly luminescent CdTe$_{0.5}$Se$_{0.5}$/Cd$_{0.5}$Zn$_{0.5}$S core/shell QDs has been presented. CdSe, CdTe, and CdTe$_{0.5}$Se$_{0.5}$ cores were first fabricated by a less toxic organic synthesis. Experimental results indicated that the size and PL properties depended strongly on the injection speed of anion precursors. CdSe and CdTe$_{0.5}$Se$_{0.5}$ cores exhibited high stability, while the PL of CdTe cores was quenched after 2 days. Subsequently, CdTe$_{0.5}$Se$_{0.5}$ cores were coated with Cd$_{0.5}$Zn$_{0.5}$S shells at relatively low temperature by using metal acetate and TOPS. This method has significant advantages: being less toxic, insensitive to air and moisture, easier to purify, and provide highly monodispersed QDs with a high PL efficiency and NIR emission. Namely, the Cd$_{0.5}$Zn$_{0.5}$S shell makes a CdTe$_{0.5}$Se$_{0.5}$ core a significant red shift of both absorption and PL spectra with reaction time. Experimental results indicated that the lower deposition temperature played a critical role for overgrowing shell material around the cores and getting high PL efficiency of the core/shell QDs. The emission wavelength from the core/shell QDs can span

Figure 6 TEM images CdTe$_{0.5}$Se$_{0.5}$/Cd$_{0.5}$Zn$_{0.5}$S core/shell QDs shown in Table 4. (**a**) Sample 6–5 and (**b**) sample 6–9. The core/ shell QDs were prepared by using sample 6.
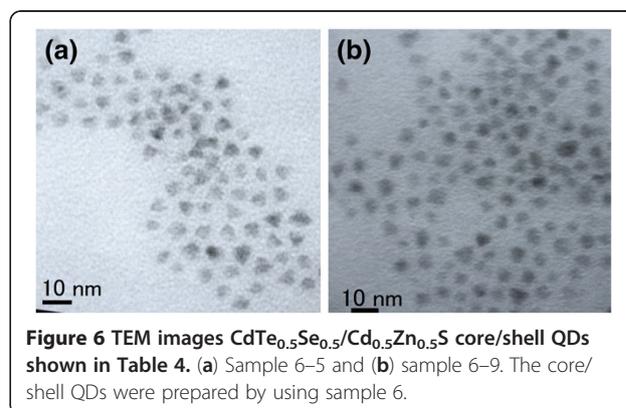
from the initial PL of the $CdTe_{0.5}Se_{0.5}$ core to 735 nm, which is achieved through the construction of the structure of a composite shell on a composite core. Because of tunable PL wavelength, high PL efficiency, and high stability, we expect that these core/shell QDs would be promising biomedical fluorophores for ultrasensitive, multicolor, and multiplexing applications, especially in *vivo* biomedical imaging applications.

Competing interest

The authors declare that they have no competing interests.

Authors' contributions

PY carried out most of the experiment. SW measured the spectrum and analyzed the data. NM provided the research conditions and did the experiment and discussion together. All authors read and approved the final manuscript.

Author details

[1]Health Research Institute, National Institute of Advanced Industrial Science & Technology (AIST), Hayashi-cho, Takamatsu-city, Kagawa 761-0395, Japan. [2]School of Material Science and Engineering, University of Jinan, Jinan 250022, People's Republic of China.

References

1. Somers RC, Bawendi MG, Nocera DG: **CdSe nanocrystal based chem-/bio-sensors.** *Chem Soc Rev* 2007, **36**:579–591.
2. Tessler N, Medvedev V, Kazes M, Kan SH, Banin U: **Efficient near-infrared polymer nanocrystal light-emitting diodes.** *Science* 2002, **295**:1506–1508.
3. Peng L, Wang Y, Dong Q, Wang Z: **Passivated ZnSe nanocrystals prepared by hydrothermal methods and their optical properties.** *Nano-Micro Lett* 2010, **2**:190–196.
4. Wu J, Wang ZM, Dorogan VG, Li S, Mazur YI, Salamo JG: **Nanoscale, near infrared broadband emission of $In_{0.35}Ga_{0.65}As$ quantum dots on high index GaAs surfaces.** *Nanoscale* 2011, **3**:1485–1488.
5. Gao J, Chen K, Xie R, Xie J, Yan Y, Cheng Z, Peng X, Chen X: **In vivo tumor-targeted fluorescence imaging using near-infrared non-cadmium quantum dots.** *Bioconjugate Chem* 2010, **21**:604–609.
6. Karthick Raja Namasivayam S, Gnanendra Kumar E, Reepika R: **Synthesis of silver nanoparticles by *Lactobaciluus acidophilus* 01 strain and evaluation of its *in vitro* genomic DNA toxicity.** *Nano-Micro Lett* 2010, **2**:160–163.
7. Rogach AL, Franzl T, Klar TA, Feldmann J, Gaponik N, Lesnyak V, Shavel A, Eychmuller A, Rakovich YP, Donegan JF: **Aqueous synthesis of thiol-capped CdTe nanocrystals: state-of-the-art.** *J Phys Chem C* 2007, **111**:14628–14637.
8. Jiang W, Singhal A, Zheng J, Wang C, Chan WCW: **Optimizing the synthesis of red- to near-IR-emitting CdS-capped $CdTe_xSe_{1-x}$ alloyed quantum dots for biomedical imaging.** *Chem Mater* 2006, **18**:4845–4854.
9. Yang P, Ando M, Taguchi T, Murase N: **Highly luminescent $CdSe/Cd_xZn_{1-x}S$ QDs with narrow spectrum and widely tunable wavelength.** *J Phys Chem C* 2011, **115**:14455–14460.
10. Pons T, Lequeux N, Mahler B, Sasnouski S, Fragola A, Dubertret B: **Synthesis of near-infrared-emitting, water-soluble CdTeSe/CdZnS core/shell quantum dots.** *Chem Mater* 2009, **21**:1418–1424.
11. Yang P, Murase N, Suzuki M, Hosokawa C, Kawasaki K, Kato T, Taguchi T: **Bright, non-blinking, and less-cytotoxic SiO_2 beads with multiple CdSe/ZnS nanocrystals.** *Chem Commun* 2010, **46**:4595–4597.
12. Yang P, Ando M, Murase N: **Highly luminescent $CdSe/Cd_xZn_{1-x}S$ quantum dots coated with thickness-controlled SiO_2 shell through silanization.** *Langmuir* 2011, **27**:9535–9540.
13. Sheng W, Kim S, Lee J, Kim SW, Jensen K, Bawendi MG: **In-situ encapsulation of quantum dots into polymer microspheres.** *Langmuir* 2006, **22**:3782–3790.
14. Murase N, Li C: **Consistent determination of photoluminescence quantum efficiency for phosphors in the form of solution, plate, thin film, and powder.** *J Lumin* 2008, **128**:1896–1903.
15. Zeng Q, Kong X, Sun Y, Zhang Y, Tu L, Zhao J, Zhang H: **Synthesis and optical properties of type II CdTe/CdS core/shell quantum dots in aqueous solution via successive ion layer adsorption and reaction.** *J Phys Chem C* 2008, **112**:8587–8593.
16. Regulacio MD, Han M: **Composition-tunable alloyed semiconductor nanocrystals.** *Acc Chem Res* 2010, **43**:621–630.
17. Swafford LA, Weigand LA, Bowers MJ II, McBride JR, Rapaport JL, Watt TL, Dixit SK, Feldman LC, Rosenthal SJ: **Homogeneously alloyed CdS_xSe_{1-x} nanocrystals: synthesis, characterization, and composition/size-dependent band gap.** *J Am Chem Soc* 2006, **128**:12299–12306.
18. Zhong XH, Feng YY, Knoll W, Han MY: **Alloyed $Zn_xCd_{1-x}S$ nanocrystals with highly narrow luminescence spectral width.** *J Am Chem Soc* 2003, **125**:13559–13563.
19. Talapin DV, Mekis I, Götzinger S, Kornowski A, Benson Q, Weller H: **CdSe/CdS/ZnS and CdSe/ZnSe/ZnS core-shell-shell nanocrystals.** *J Phys Chem B* 2004, **108**:18826–18831.
20. Ouyang JY, Ratcliffe CI, Kingston D, Wilkinson B, Kuijper J, Wu XH, Ripmeester JA, Yu K: **Gradiently alloyed $Zn_xCd_{1-x}S$ colloidal photoluminescent quantum dots synthesized via a noninjection one-pot approach.** *J Phys Chem C* 2008, **112**:4908–4919.
21. Sun M, Yang X: **Phosphine-free synthesis of high-quality CdSe nanocrystals in noncoordination solvents: "activating agent" and "nucleating agent" controlled nucleation and growth.** *J Phys Chem C* 2009, **113**:8701–8709.
22. Empedocles SA, Bawendi M: **Spectroscopy of single CdSe nanocrystallites.** *Acc Chem Res* 1999, **32**:389–396.
23. Dabbousi BO, Rodriguez-Viejo J, Mikulec FV, Heine JR, Mattoussi H, Ober R, Jensen KF, Bawendi MG: **(CdSe)ZnS core-shell quantum dots: synthesis and characterization of a size series of highly luminescent nanocrystallites.** *J Phys Chem B* 1997, **101**:9463–9475.